

## Ultrahigh resolution study of collective modes in $^{158}\text{Gd}$

H. G. Börner,<sup>1</sup> M. Jentschel,<sup>1</sup> N. V. Zamfir,<sup>2,3</sup> R. F. Casten,<sup>2</sup> M. Krťicka,<sup>4</sup> and W. Andrejtscheff<sup>5</sup>

<sup>1</sup>*Institut Laue-Langevin, F-38042 Grenoble, France*

<sup>2</sup>*Wright Nuclear Structure Laboratory (WNSL), Yale University, New Haven, Connecticut 06520*

<sup>3</sup>*Clark University, Worcester, Massachusetts 01610*

<sup>4</sup>*Charles University, CZ-18000 Prague, Czech Republic*

<sup>5</sup>*Bulgarian Academy of Sciences, Institute for Nuclear Research and Nuclear Energy, 1784 Sofia, Bulgaria*

(Received 13 November 1998)

Ultraprecise energies and absolute  $B(E2)$  values associated with  $K=0^+$  excitations in  $^{158}\text{Gd}$ , measured with the GRID technique, reveal significant information relating to the possible existence or absence of two-phonon vibrational excitations in deformed nuclei. A strong  $B(E2:K=0_2^+ \rightarrow \gamma)$  is observed but reflects band mixing rather than a  $\gamma\gamma$  mode. For the  $K=0_3^+$  band, measurement of precise  $\gamma$  transition energies shows that suggested existing placements of strong deexcitation transitions are incorrect and that there is, again, no evidence for  $\gamma\gamma$ -phonon character in this band either. A weak  $B(E1:K=1^- \rightarrow K=0_1^+)$  value is interpreted in terms of the microscopic structure of  $K=0^-$  and  $K=1^-$  excitations. [S0556-2813(99)06705-9]

PACS number(s): 23.20.Lv, 23.20.Js, 27.70.+q, 29.30.Kv

### I. INTRODUCTION

The question of whether multiphonon states exist in nuclei or whether their strength is severely fragmented is an important issue closely linked to the role of the Pauli principle in a strongly interacting fermionic quantal system with low degeneracy orbits. In such a system, phonon modes can be described as linear superpositions of particle-hole states [1]. At some point in the construction of successive many-phonon excitations, either a source or a destination orbit will be emptied or filled, respectively, and therefore blocked. The wave function for such an excitation will be modified compared to that for an exact superposition of  $N$  phonons. Long before this, partial occupancies can be expected to modulate the phonon properties. It has therefore been of some surprise, and has had strong theoretical repercussions, that a number of multiphonon states (both in the low-energy spectrum and of giant resonance character) have been discovered in recent years.

In low-lying states of spherical nuclei, levels with significant amplitudes for up to five quadrupole phonons have been identified in  $^{114}\text{Cd}$  (Ref. [2]), and a number of three-phonon states found in other near-closed shell nuclei. In deformed nuclei, the first example [3] of a two-phonon vibrational excitation observed is a  $K=4^+$  state in  $^{168}\text{Er}$  with a substantial amplitude for double  $\gamma$ -vibrational character. Other examples of  $K=4^+$  modes with substantial  $\gamma\gamma$  character have since been discovered [4–7]. The 1943 keV level in  $^{166}\text{Er}$ , discovered in  $(n, n' \gamma)$  [7] and Coulomb excitation [5], has been suggested [7] as having a large amplitude for a two-phonon  $\gamma\gamma$  excitation with  $K=0^+$ . Double phonon states involving two different phonon modes, such as  $2^+ \otimes 3^-$  excitations, or those involving mixed symmetry states ( $2^+ \otimes 2_{ms}^+$ ), are known in the Ba isotopes [8,9]. Finally, double phonon structures have begun to be observed in giant resonance excitations [10].

One signature of multiphonon levels (of phonon number  $N_{ph}$ ) is allowed decay to  $(N_{ph}-1)$ -phonon states, combined

with forbidden transitions to zero phonon levels [indeed, to any levels with  $(N_{ph}-2)$  or fewer phonons]. However, preferential decay of an excited  $K=0^+$  state to the  $\gamma$  vibration does not in itself establish 2- $\gamma$  phonon character. It is possible to imagine two-quasiparticle amplitudes in the  $\gamma$ -band wave functions such that  $K=0^+$  states of two-quasiparticle, or even of pairing or  $\beta$ -vibrational character, could also have such a decay preference. A better test of two-phonon character requires the measurement of absolute transition rates, that is,  $B(E2:J_{K=0^+} \rightarrow J_\gamma)$  values. If these are collective then a two-phonon interpretation should be considered (but still not assured—see below).

An obvious prerequisite for studying candidate levels for multiphonon states in the excitation energy range  $\sim 1.2$ – $2.0$  MeV, is accurate  $\gamma$ -ray transition placements in the level scheme. The level density increases rapidly in this excitation energy region and the likelihood of misplaced  $\gamma$ -ray transitions increases accordingly. Accurate transition placements are usually achieved by  $\gamma$ - $\gamma$  coincidence measurements with high efficiency multidetector arrays. However, an equally powerful technique is ultraprecise  $\gamma$ -ray energy measurements (with accuracies of a few eV) since, then, the possibility of incorrect placements (incorrect Ritz combinations) is virtually eliminated.

The use of the ultrahigh resolution GAMS4 flat crystal spectrometer at the ILL in Grenoble provides the opportunity to obtain both highly precise transition energies and absolute  $B(E2)$  values for transitions observed in the  $(n, \gamma)$  process. The  $B(E2)$  values are obtained from lifetime measurements using the GRID ( $\gamma$ -ray induced Doppler) technique [11] in which Doppler broadening is measured for a deexcitation  $\gamma$  ray emitted while a nucleus is recoiling due to the prior emission of another  $\gamma$  ray following neutron capture. Since such recoil energies are minuscule (a few eV), the observation of broadening in transitions of, say, 1 MeV energy, requires extraordinarily high resolution which, in turn, allows sensitive tests of transition placements as well. Absolute transition energies were measured with the GAMS4 spectrometer by detection of the Bragg diffraction angle of the  $\gamma$  ray of inter-

est from Si crystals. The precision energy measuring capability of this spectrometer results from the incorporation of two unique features. First, the crystals are nearly perfect specimens whose lattice spacings have been measured with an uncertainty of  $5 \times 10^{-8}$ . Second, the diffraction angles are measured with sensitive interferometers which are instrumented for frequent absolute angle calibrations which are—if sufficient statistics is gathered—robust at the  $10^{-7}$  level. The technique and the GAMS4 spectrometer have been described elsewhere [11,12].

The purpose of this paper is to present results from a GRID study of  $^{158}\text{Gd}$ . First,  $\gamma$ -ray energies in  $^{158}\text{Gd}$  were measured. Their level of precision allows us to test the existing level scheme. It was found that the accepted decay of the second excited  $K=0^+$  band (the  $0_3^+$  band) to the  $\gamma$  band is, in fact, not correct. Secondly, lifetimes of states in the  $K=0_2^+$  and  $0_3^+$  bands were measured. A strong  $B(E2:K=0_2^+ \rightarrow \gamma)$  band value was found. However, this value does not imply  $\gamma\gamma$  phonon character since it can be fully explained as a consequence of band mixing. The large  $B(E2)$  value results since the  $\gamma$  and  $K=0_2^+$  bands are uncommonly close in energy:  $\Delta E(2_{K=0_2^+}^+ - 2_\gamma^+)$  is 73 keV. (For simplicity we will use the notation  $J_\gamma^+$  for members of the lowest  $K=2^+$  band and  $J_1^+$  for the ground band.) Finally, the  $B(E1:1_{K=1^-}^- \rightarrow 0_1^+)$  value was measured for the lowest  $K=1^-$  band. This is only the second nucleus in this mass region where this quantity is known and its value demonstrates the relative hindrance of  $K=1^- \rightarrow K=0^+$ ,  $1^- \rightarrow 0^+ E1$  transitions compared to  $K=0^- \rightarrow K=0^+$ ,  $1^- \rightarrow 0^+ E1$  transitions.

II. EXPERIMENT AND RESULTS

In this experiment, the large thermal neutron capture cross section of  $\approx 2.42 \times 10^5$  b was exploited to give prolific production of  $^{158}\text{Gd}$  on a target of natural Gd. The Doppler broadening was measured by carefully scanning the energy of the decay  $\gamma$  rays of interest. This broadening results from a convolution of the initial recoil velocity distribution of the excited nuclei, the slowing down process, and the level lifetime. Any transition from a level can be used for the lifetime measurement. Usually, this is one of the higher energy  $\gamma$  rays to the ground state band since the  $E_\gamma^5$  factor enhances the intensity of such transitions relative to lower energy de-excitation  $\gamma$  rays even if their  $E2$  matrix elements are small. From the known  $E2$  branching ratios, the matrix elements of lower energy transitions can then be extracted. Figure 1 shows two examples of the data—the Doppler broadened line shape for the 1141 keV transition and the energy scan for the 1187 keV transition. The latter shows an energy resolution at 1.2 MeV of  $\sim 6$  eV. Two transitions  $\sim 22$  eV apart are easily separated. The widths in Fig. 1(a) are primarily due to Doppler broadening and the excess width compared to the instrumental line width leads to the extraction of a measured lifetime.

In addition to the Doppler width due to the recoil velocity there is a small Doppler broadening of the peak due to the thermal vibrational motion of atoms in the target (the  $^{158}\text{Gd}$  target was located in the reactor core at a temperature of  $\sim 970$  K). This thermal motion can be calibrated using tran-

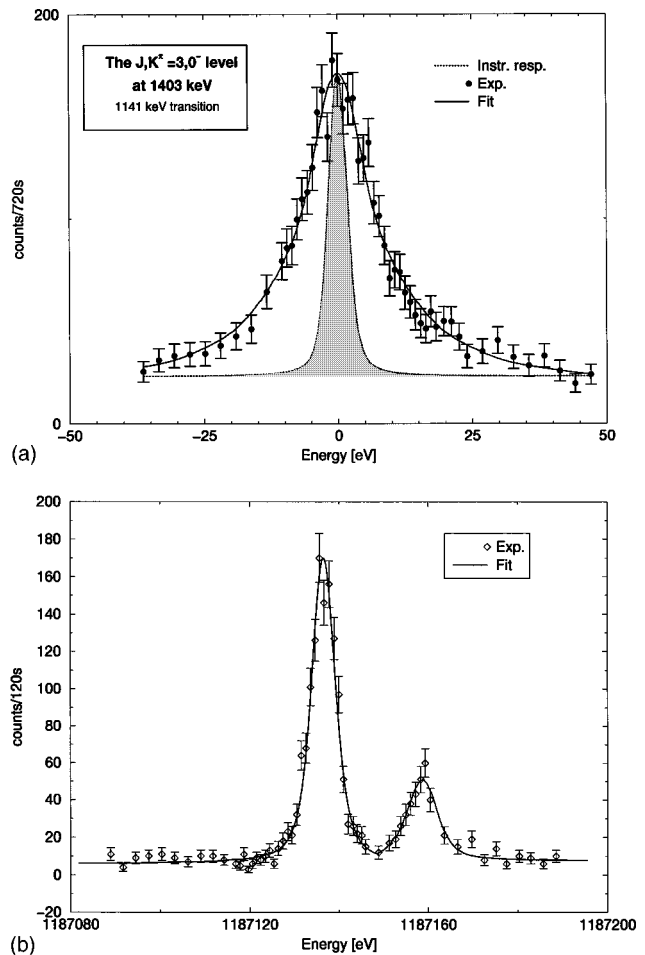


FIG. 1. Two examples of the data: (a) The Doppler broadened line shape for the 1141 keV transition. The dotted line shows the instrumental line width. The solid line is a fit to the data that incorporates Doppler broadening due to the finite lifetime. (b) Example of the energy determination of measured  $\gamma$  ray lines. The figure shows a small region of the spectrum with the 1187.1365 keV  $\gamma$  ray energy measured here in third order of reflection along with a neighboring weaker transition 22 eV apart (1187.1583 keV) which belongs to  $^{156}\text{Gd}$ .

sitions of known lifetimes. It is easy therefore to extract the Doppler contribution to the width due to the finite level lifetime. The major uncertainty in extracting level lifetimes with the GRID technique is not due directly to the measurement itself, but rather to estimating the initial recoil velocity distribution of  $^{158}\text{Gd}$  nuclei at the time of population of the levels of interest and, in particular, its dependence on the energy distribution of the feeding  $\gamma$  rays and the lifetimes of intermediate levels.

A statistical decay calculation can be done to estimate this but a safer, and more conservative, approach is to extract upper and lower lifetime limits for each level from extreme assumptions about the population routes and intensities. The highest recoil velocities will naturally be given by assuming that all unobserved feeding is via a two-step cascade from the neutron capture state (the amount of one-step feeding is known) with intermediate level lifetime  $\tau=0$ . Then, for depopulating  $\gamma$  rays the supposed initial Doppler broadening will be maximum and any given measured broadening (less than the maximum) corresponds to the longest slowing down

TABLE I. Mean lifetimes measured in this work deduced from extreme feeding assumptions and from statistical model calculations ( $\tau_{\text{FFPA}}$ ).

$J, K^\pi$	$E_x$ (keV)	$\tau_{\min} - \tau_{\max}$ (ps)	$\tau_{\text{FFPA}}^{\text{a}}$ (ps)	$\tau_{\text{lit}}$ (ps)	$\tau = 0.88\tau_{\max}^{\text{b}}$ (ps)
$2,2_1^+$	1187	0.498 – 1.000	$0.712^{+0.134}_{-0.096}$	0.88(6) <sup>c</sup>	0.88
$3,2_1^+$	1266	0.555 – 1.783	$1.019^{+0.134}_{-0.112}$		1.6
$4,2_1^+$	1358	0.409 – 1.151	$0.918^{+0.148}_{-0.121}$		1.0
$0,0_2^+$	1196	1.855 – 9.035	$3.867^{+2.288}_{-1.056}$		8.0
$2,0_2^+$	1260	1.406 – 5.899	$2.339^{+0.629}_{-0.414}$	5.2(4) <sup>d</sup>	5.2
$4,0_2^+$	1407	0.529 – 1.868	$1.076^{+0.090}_{-0.092}$		1.6
$0,0_3^+$	1452	0.208 – 1.734	$1.033^{+0.578}_{-0.265}$		1.5
$2,0_3^+$	1517	0.277 – 1.478	$0.783^{+0.407}_{-0.198}$	2.0(2) <sup>d</sup>	1.3
$1,1_1^-$	977	0.899 – 2.341	$0.938^{+0.181}_{-0.135}$		2.06
$2,1_1^-$	1024	>5	>20		>5
$3,1_1^-$	1042	0.293 – 0.565	$0.410^{+0.031}_{-0.030}$	0.78(22) <sup>c</sup>	0.50
$4,1_1^-$	1159	1.549 – 5.452	$2.535^{+0.863}_{-0.469}$		4.8
	1176	0.216 – 0.518	$0.286^{+0.031}_{-0.027}$		0.46
$1,0_1^-$	1264	<0.053	$0.0415^{+0.0036}_{-0.0033}$	0.019(4) <sup>e</sup>	<0.047
$3,0_1^-$	1403	<0.078	$0.0337^{+0.0035}_{-0.0033}$		<0.069
$2,2_1^-$	1793	0.340 – 10.349			9.1

<sup>a</sup> $\tau$  deduced from statistical model calculations (FFPA).

<sup>b</sup>See text. For the purposes of discussion we use these values.

<sup>c</sup>From Ref. [14].

<sup>d</sup>From Ref. [15].

<sup>e</sup>From Ref. [16].

time before  $\gamma$ -ray emission and therefore to the longest lifetime. The limit, which is the safest and easiest to estimate, is the main one of interest here since we are looking to test for *collective* transitions. Any lifetimes shorter than the long lifetime limit correspond to larger, more collective,  $B(E2)$  values.

The lower limit on the lifetimes [upper limit on the  $B(E2)$  values] comes from assuming that all the feeding of each level comes from a state of effectively infinite lifetime (hence the nucleus emitting the feeding  $\gamma$  ray has no initial recoil velocity) at the lowest possible energy consistent with the known level scheme (i.e., about 2 MeV in  $^{158}\text{Gd}$ ). In practice we use a slight variant of this extreme scenario dictated by the use of known, but unplaced,  $\gamma$  rays. This produces only a small change and, in any case, as we shall see, we have independent evidence that the actual lifetimes are near the upper limits described above. Table I lists the lifetimes measured, giving the extreme conservative limits, the values from a statistical model calculation, and those based on the calibration procedure described next. The statistical model calculation [13] was incorporated into the so called fluctuating free path approach (FFPA), used here to describe the slowing down of nuclei recoiling after the emission of  $\gamma$  rays.

Within the FFPA the time interval between any pair of

successively emitted  $\gamma$  rays in a cascade is treated as a quantity randomly drawn from the exponential distribution whose average is uniquely determined by the total radiation width of the appropriate intermediate level. For a given step of a cascade the induced recoil velocity is  $v = E_\gamma/(mc)$ , where  $m$  is the mass of the recoiling atom and  $E_\gamma$  is the  $\gamma$ -ray energy. The data for individual  $\gamma$  cascades, i.e.,  $\gamma$ -ray energies and total radiation widths of the intermediate levels, are provided by simulation using the algorithm DICEBOX [13].

Only binary, classical hard-sphere collisions between the projectile atom and atoms of the sample are considered. The energy-dependent [12] hard-sphere radius is deduced from the equality of the initial kinetic energy in the center-of-mass (c.m.) system to the repulsive Born-Mayer potential. In the c.m. system the angular distribution of atoms after the collisions is understood to be isotropic and energy losses in the laboratory system are thus considered to be variable. To take into account the process of thermalization, the velocities of atoms of the sample are assumed to follow the Maxwell-Boltzmann distribution.

We first note that we are dealing with a statistical decay process following thermal neutron capture at low spin. All the levels whose lifetimes were measured occur in a rather narrow excitation energy range ( $E_x$  in 950–1800 keV compared to a neutron capture state energy of 7.9371 MeV) and

TABLE II. The  $B(E2)$  values for the decay of the  $K=2_1^+$  and  $K=0_2^+$  bands in  $^{158}\text{Gd}$ .

$J_i, K_i^\pi$	$E_{x_i}$ (keV)	$J_f, K_f^\pi$	$E_{x_f}$ (keV)	$B(E2:J_i \rightarrow J_f)^{a,b}$ $e^2 b^2$	W.u.
$2,2_1^+$	1187	$0,0_1^+$	0	0.017(2)	3.3(6)
		$2,0_1^+$	80	0.030(4)	5.9(7)
		$4,0_1^+$	261	0.0013(2)	0.27(4)
$3,2_1^+$	1265	$2,0_1^+$	80	0.017(1)	3.3(2)
		$4,0_1^+$	261	0.010(1) <sup>c</sup>	2.0(2) <sup>c</sup>
$4,2_1^+$	1358	$2,0_1^+$	80	0.005(1)	1.1(1)
		$4,0_1^+$	261	0.037(2)	7.4(4)
		$2,2_1^+$	1187	0.57(4)	112(7)
$0,0_2^+$	1196	$2,0_1^+$	80	0.0057(4)	1.1(1)
$2,0_2^+$	1260	$0,0_1^+$	0	0.0016(1)	0.30(2)
		$4,0_1^+$	261	0.0069(4)	1.3(1)
		$2,0_1^+$	80	0.0066(4)	1.3(1)
$4,0_2^+$	1407	$4,0_1^+$	261	0.0037(6)	0.7(1)
		$6,0_1^+$	539	0.016(1)	3.1(2)
		$2,2_1^+$	1187	0.065(10)	13(2)
		$3,2_1^+$	1265	0.24(10) <sup>c</sup>	48(19) <sup>c</sup>
		$2,0_2^+$	1260	2.3(2)	447(47)

<sup>a</sup>Obtained using the  $\tau$  listed in the last column of Table I and intensities of  $\gamma$ -ray transitions from Ref. [17].

<sup>b</sup>Uncertainties of  $\gamma$ -ray intensities of Ref. [17] only. These uncertainties therefore reflect the uncertainties in relative  $B(E2)$  values from each level. For absolute  $B(E2)$  values the uncertainties in the present measurements need to be added.

<sup>c</sup>If pure  $E2$ .

have fairly similar measured lifetimes (the upper limits range in most cases from  $\sim 0.5$ –10 ps). The  $2_\gamma^+$  level at 1187 keV has a known lifetime (see  $\tau_{\text{lit}}$  values in Table I)  $\tau=0.88(6)$  ps [14] based on Coulomb excitation measurements of McGowan and Milner [15]. Our range is 0.498–1.00 ps. The  $2_{K=0}^+$  level at 1260 keV has a known lifetime of 5.2(4) ps [15], while our range is 1.406–5.899 ps. Both of these well-established lifetimes correspond to 0.88 times our upper limit lifetime. We therefore adopt for simplicity of calculating  $B(E2)$  values, and in a sense to guide the eye, a calibration factor of 0.88 and include the corresponding lifetimes in Table I. Evidently, only the limits given in column three give model independent values for the lifetimes.

Comparison with literature values for other levels with known lifetimes shows reasonable agreement. Our lifetime of  $\tau=0.50$  ps is within uncertainties of the known value [ $\tau=0.78(22)$  ps] for the  $3^-$  level at 1042 keV [14]. Our lifetime of  $\tau=1.3$  ps is also in acceptable concord with existing data ( $\tau=2.0(2)$  ps) for the 1517 keV  $2_{K=0}^+$  level [15]. For the 1264 keV  $1^-$  level our upper limit is consistent with the value calculated using the  $B(E1)$  values from  $(\gamma, \gamma')$  data [16].

The lifetime results in Table I show many values measured for the first time, giving information on transitions from the  $\gamma$  band, the  $K=0_2^+$  and  $0_3^+$  bands and  $K=0^-, 1^-,$  and  $2^-$  negative parity bands. Table II gives the  $B(E2)$  values for the decay of the  $K=2_1^+$  and  $K=0_2^+$  bands in  $^{158}\text{Gd}$  deduced from the lifetime results. Table III gives a number of highly precise transition energies measured in this

TABLE III. Highly precise transition energies measured in this work and the implied  $J_i K_i$  values and level energies,  $E_{x_i}$ .

$J_i, K_i^\pi$	$J_f, K_f^\pi$	Measured <sup>a</sup> $E_{\text{tr}}$ (keV) <sup>b</sup>	$E_{x_i}$ (keV) <sup>b</sup>
$2,0_1^+$		977.147(2)–897.634(2)	79.513(3)
$4,0_1^+$		1259.870(3)–998.412(2)	261.458(4)
$4,0_1^+$	$2,0_1^+$	181.943(1)	261.456(3)
		mean	261.457(3)
$1,1_1^-$	$0,0_1^+$	977.147(2)	977.147(2)
$2,1_1^-$	$2,0_1^+$	944.184(2)	1023.697(4)
$3,1_1^-$	$2,0_1^+$	962.125(2)	1041.638(4)
$4,1_1^-$	$4,0_1^+$	897.509(2)	1158.966(3)
$2,2_1^+$	$0,0_1^+$	1187.141(3)	1187.141(3)
$2,0_2^+$	$0,0_1^+$	1259.870(3)	1259.870(3)
		998.412(2)	1259.869(3)
		mean	1259.870(2)
$1,0_1^-$	$0,0_1^+$	1263.514 (3)	1263.514(3)
$3,2_1^+$	$2,0_1^+$	1186.007(3)	1265.520(4)
$4,2_1^+$	$4,0_1^+$	1097.011(3)	1358.468(3)
$3,0_1^-$	$4,0_1^+$	1141.481(3)	1402.938(4)
$4,0_2^+$	$2,0_1^+$	1327.190(3)	1406.703(4)
$2,0_3^+$	$2,0_1^+$	1437.967(3)	1517.480(4)
		475.840(1)	1517.478(4)
	$3,1_1^-$	mean	1517.479(3)

<sup>a</sup>Present experiment. Due to recoil correction included here these energies are a few electron volts higher than the measured  $\gamma$ -ray energies (e.g., compare the 1187.136 keV line in Fig. 1 with the entry 1187.141 keV here).

<sup>b</sup>Uncertainties are on the last digit, that is, in eV.

work and the implied level energies in  $^{158}\text{Gd}$ . Figure 2 shows a partial level scheme for  $^{158}\text{Gd}$  exhibiting the key transitions of interest and summarizing the present results as well.

For the discussion to follow, it is critical to note that the  $\gamma$ -ray energy precision extends not only to the relative errors on transition energies but to the absolute energy scale as well. This scale is fixed by the known crystal lattice spacing and by the absolute diffraction angle calibration. The combination of these two uncertainties gives a scale that is accurate at the  $10^{-7}$  level. Additionally to that one has to include an uncertainty which is essentially related to statistics and which is here in the order of  $10^{-6}$ , that is, at most 1 eV for a 1 MeV transition, and proportionately less for lower energy transitions. The scale is fixed and not adjustable. We will return to this point below.

Many of the results in Table III come from transitions involving the  $2_1^+$  and  $4_1^+$  levels, whose energies therefore need to be determined first. The energy of the  $2_1^+$  level at 79.513 (3) keV was determined from the energy difference of the transitions of energies 977.147 (2) keV and 897.634 (2) keV from the 977 keV level to the ground state and  $2_1^+$  level, respectively. The energy of the  $4_1^+$  level was determined from the 1259.870 (3) keV and 998.412 (2) keV transitions from the 1260 keV  $2_1^+$  level to the ground state and  $4_1^+$  level, respectively. A test of the energies of the  $2_1^+$  and  $4_1^+$  levels is provided by the measured energy of the 181.943 keV transition between them. The remaining results in Table III now follow. Note that we have two independent measurements of the energies of the 1260 and 1517 keV levels which

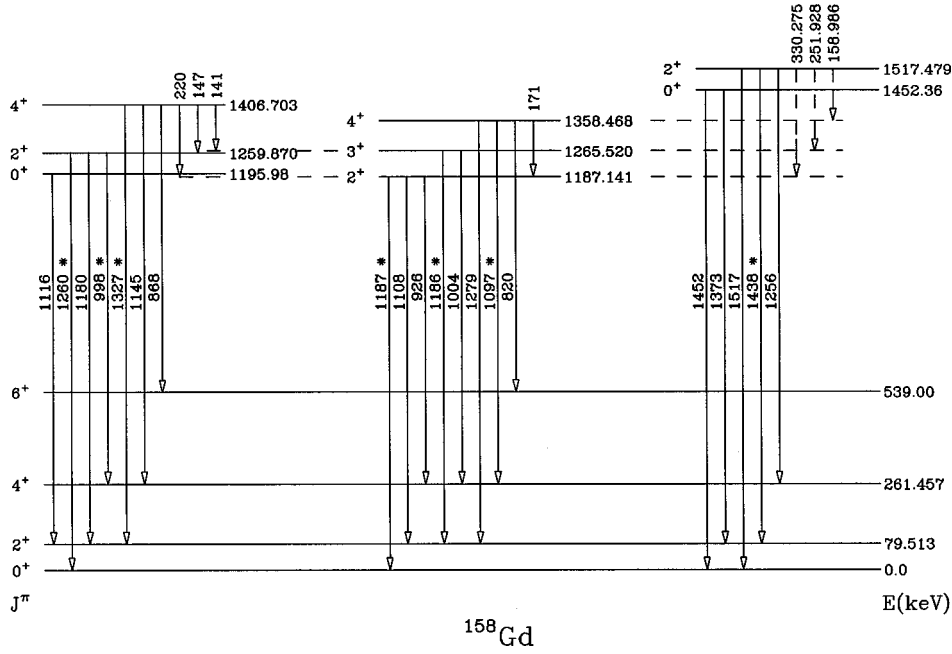


FIG. 2. Partial level scheme for  $^{158}\text{Gd}$  exhibiting key transitions connecting positive parity states. The uncertainties on these level energies are 3–4 eV. The  $\gamma$ -ray transitions shown in this figure that were actually measured here with the GAMS4 spectrometer are marked with an asterisk. Other transitions measured here include the 475.840 keV line connecting the 1517 keV level with the 977 keV  $1^-$  state as well as several transitions from negative parity states (see Table III). The precise level energies shown with three digits following the decimal point were determined from all the data, including transitions (e.g., connecting these levels with negative parity states) not shown. No  $\gamma$  rays from the 539, 1196, and 1452 keV levels were measured here and so their energies are rounded to two digits. Cross checks of their energies are consistent with the present results. To avoid clutter only nominal  $\gamma$ -ray energies are shown, with the exception of the low-energy transitions from the  $2_{K=0_3}^+$  state at 1517 keV which are given to all known accuracy so that the energy discrepancies in these placements are easily seen. For these three transitions we give the scaled (factor 1.000035)  $\gamma$ -ray energies from Ref. [17] (see text). The recoil corrections for such low-energy  $\gamma$  rays are  $<1$  eV. These transitions are dotted because the present data show them to be misplaced in the level scheme.

differ by 1 and 2 eV, respectively, and are therefore well within errors. Table IV gives several precise transition energies relating to the important  $2_{K=0}^+$  level at 1517 keV (see text below for further discussion). The energy uncertainties for transition energies in Table III and level energies ( $E_{x_i}$ ) in Tables III and IV include all sources of error—uncertainties from the absolute energy scale, from statistics, and from peak fitting.

We note in passing one other point concerning precise level energies and transition placements. Our deduced energy for the 977 keV level is higher than in Ref. [17] and the transition from the 1196 keV level to the 977 keV level is better fit with a transition of 218.82 keV (unplaced in Ref. [17]) than with the 219.02 keV transition assigned to this transition in that work. In all other regards our level scheme shows the same transitions as that of Ref. [17].

### III. DISCUSSION

We will focus here on three results of particular interest: The decay of the first excited  $K=0^+$  band at 1196 keV, transition placements for the decay of the second excited  $K=0^+$  band at 1452 keV (in particular for the  $2^+$  level at 1517 keV) and the  $B(E1)$  values for the decay of the negative parity bands. First, though, we note that our measurements also provide the first absolute  $B(E2)$  values (see Table II) for the decay of the  $3_\gamma^+$  and  $4_\gamma^+$  states:  $B(E2:3_\gamma^+ \rightarrow 2_1^+) = 0.017 e^2 b^2$ ,  $B(E2:4_\gamma^+ \rightarrow 2_1^+) = 0.005 e^2 b^2$ , and  $B(E2:4_\gamma^+ \rightarrow 2_\gamma^+) = 0.57 e^2 b^2$ . Earlier, in a four-band mixing analysis Greenwood *et al.* [17] had estimated  $B(E2:3_\gamma^+ \rightarrow 2_1^+)$  and  $B(E2:4_\gamma^+ \rightarrow 2_1^+)$  values of  $0.03 e^2 b^2$  and  $0.006 e^2 b^2$ , respectively, assuming that the  $B(E2:4_\gamma^+ \rightarrow 2_\gamma^+)$  had a value of  $0.6 e^2 b^2$  obtained by calculating the intraband  $B(E2:4_\gamma^+ \rightarrow 2_\gamma^+)$  value from the  $B(E2:2_1^+ \rightarrow 0_1^+)$  value assuming the rotational formula. This assumption, upon which their multiband mixing calculation relies, and therefore the results that followed from it, are thus validated by the present results.

The first key results are the lifetimes of the  $0_{K=0_2}^+$  and  $4_{K=0_2}^+$  levels. These, in turn, give very strong intraband  $B(E2)$  values and  $B(E2:4_{K=0_2}^+ \rightarrow 2_\gamma^+) = 13(2)\text{W.u.}$  ( $0.065 e^2 b^2$ ) and (if pure  $E2$ )  $B(E2:4_{K=0_2}^+ \rightarrow 3_\gamma^+) = 48(19)\text{W.u.}$  ( $0.24 e^2 b^2$ ) values. Both the latter  $B(E2)$  values are large for interband transitions and would normally be considered evidence for two-phonon ( $\gamma\gamma$ ) character. However, noting that the two bands are almost degenerate [ $E(4_{K=0_2}^+) - E(4_\gamma^+) = 48$  keV] even a modest rotation-vibration interaction leads to significant band mixing. Indeed, with a spin-independent mixing matrix element of 0.6 keV and no direct  $M(E2)$  between these bands, Greenwood *et al.* [17] were able to successfully account for the  $K=0_2^+ \rightarrow \gamma$  band  $B(E2)$

TABLE IV. Possible transitions from the  $2_{K=0_3}^+$  level at 1517.479(3) keV.

$J, K^\pi$	Final Level		$E_\gamma^b$ (keV) Ref. [17]	$\Delta E_x(\text{GAMS4}) - E_\gamma$ (Ref. [17]) <sup>c</sup> (eV)
	$E_{x_f}^d$ (keV)	$\Delta E_x^a$ (keV)		
$3, 0_1^-$	1403	114.541(4)	114.544(4)	$-3_{-6}^+$
$4, 2_1^+$	1358	159.011(4)	158.986(20)	$+25_{-20}^+$
$3, 2_1^+$	1266	251.959(4)	251.928(5)	$+31_{-6}^+$
$1, 0_1^-$	1263	253.965(4)	253.952(5)	$+13_{-6}^+$
$2, 2_1^+$	1187	330.337(4)	330.275(15)	$+62_{-16}^+$
$3, 1_1^-$	1042	475.840(1) <sup>e</sup>	475.856(13)	$-16_{-13}^+$
$2, 1_1^-$	1024	493.781(4)	493.793(20)	$-12_{-20}^+$
$1, 1_1^-$	977	540.331(3)	540.349(200)	$-18_{-200}^+$
$4, 0_1^+$	261	1256.017(3)	1256.024(100)	$-7_{-100}^+$
$0, 0_1^+$	0	1517.471(3)	1517.493(110)	$-22_{-110}^+$

<sup>a</sup>Energy differences  $(1517.479 - E_{x_f} - dE_r)$  keV, where  $E_{x_f}$  are the level energies deduced from the GAMS4 data (and given in the right hand column of Table III) and  $dE_r$  are the calculated recoil energies included to allow comparison with the measured  $E_\gamma$  from Ref. [17].

<sup>b</sup>Values from Ref. [17], multiplied by 1.000035. This factor omits statistical uncertainties as these are small compared to the other uncertainties in the table (see text).

<sup>c</sup>Differences in the energies deduced from the present GAMS4 data and the  $\gamma$ -ray energies of Ref. [17]. Since the level energies deduced here are accurate to 3–4 eV, most of the uncertainty comes from the  $\gamma$ -ray energies from Ref. [17]. Note particularly that the discrepancies between  $\gamma$ -ray energies and level energy differences for the  $2, 2_1^+$  and  $3, 2_1^+$  levels are many times the uncertainties, implying (see text) that these  $\gamma$ -rays are misplaced.

<sup>d</sup>The exact energies are given in the last column of Table III.

<sup>e</sup>Measured.

values that they had assumed (which were about 60% of those that we have measured).

This is a textbook example of a case where both a large branching ratio  $B(E2:K=0_2^+ \rightarrow \gamma)/B(E2:K=0_2^+ \rightarrow 0_1^+)$  and a large *absolute* value  $B(E2:K=0_2^+ \rightarrow \gamma)$  does *not* imply a  $\gamma\gamma$  phonon character. It provides a useful cautionary note.

The second result concerns potentially large and collective  $K=0^+ \rightarrow \gamma$  band transitions, in this case from the  $2^+$  level (1517 keV) of the  $K=0_3^+$  band at 1452 keV. Greenwood *et al.* [17] used  $(d, d')$  cross sections and a DWBA analysis to estimate the absolute  $B(E2)$  values of the transitions assigned to the decay of the 1517 keV level to the  $2_\gamma^+$ ,  $3_\gamma^+$ , and  $4_\gamma^+$  levels, obtaining values 1, 26, and 35 W.u., respectively. Our measured lifetime for the 1517 keV level is actually a little shorter than the previous literature value and hence these transitions would have about 50% larger  $B(E2)$  values from our data. The last two values are astonishingly large for interband transitions. Greenwood *et al.* [17] were not able to account for them with a band mixing analysis. If instead we assume that they result from a direct  $\Delta K = 2$   $E2$  matrix element, a problem also arises since their relative  $B(E2)$  values are then strongly incompatible with the Alaga rules. Greenwood *et al.* [17] (and also McGowan and Milner [15]) therefore surmised that these  $\gamma$  rays might be misplaced although their measured energies of 330.26, 251.92, 158.98 keV fit very well with the level energies deduced from other transitions.

The results of our study confirm the known lifetime for this state (see Table I) and hence the large  $B(E2)$  values (assuming the transitions are correctly placed). However, our ultraprecise  $\gamma$ -ray energy measurements give new values for the relevant level energies (see Table III) which allows us to

reassess the decay of the 1517 keV level. Construction of a level scheme from  $\gamma$ -ray energies involves both a relative and an absolute calibration of the  $\gamma$ -ray energies. A given level scheme (a set of  $\gamma$ -ray placements) is, of course, unaffected by a scaling of all the absolute energies. A consistent absolute scale is, however, necessary if data from different experiments are involved. As we have noted, our absolute energy scale is fixed at the  $10^{-6}$  or better ( $\leq 1$  eV) level. The calibration of the curved crystal spectrometer in Ref. [17] was obtained by normalizing to a previous measurement (Ref. 38 of Ref. [17]) of the 79 keV  $2_1^+ \rightarrow 0_1^+$  transition in  $^{158}\text{Gd}$  itself. Therefore, the calibration of Ref. [17] can differ from ours, due to uncertainties in that energy standard, by some factor. However, we stress that factor is wavelength (i.e.,  $\gamma$ -ray energy) independent: it is a single factor for the entire spectrum. Comparison of the precise level energies deduced from our data in Table III with those of Ref. [17] shows that  $\gamma$ -ray energies in the latter should be scaled by a uniform factor of 1.000035(12). Doing this, and comparing the energies for  $\gamma$  rays from the 1517 keV level from Ref. [17] with the precise level energy differences deduced here, we get the results in Table IV. These results show excellent overall consistency. Similar comparisons for a dozen other levels also show complete consistency well within the combined errors. Of 32 level energy differences only one has a  $3\sigma$  deviation and only two have  $2\sigma$  deviations. Moreover, in these cases the deviations are at the  $\sim 10$  eV level. However, Table IV shows a clear discrepancy for the 330.275 and 251.928 keV  $\gamma$  rays. The respective energy deviations are 62(16) and 31(6) eV. One could, of course, avoid this discrepancy by renormalizing the energy scale of Ref. [17]. However, in that case, the remainder of the level scheme

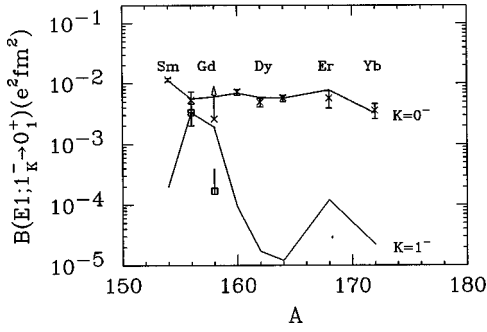


FIG. 3.  $B(E1; 1^- \rightarrow 0^+_1)$  values in the deformed rare earth region. Squares denote transitions originating in  $K=1^-$  bands and crosses refer to  $K=0^-$ . The data for  $^{158}\text{Gd}$  are from the present measurement. The error bars reflect the entire range of allowed  $\tau$  values for Table I. The other data are from Nucl. Data Sheets. The lines connect the IBA predictions [18].

would be in disagreement with the precise energies and energy scale defined here. Therefore, one is forced to conclude that, due to much higher precision in level energies obtained with GAMS4, the 330 and 251 keV  $\gamma$  rays can no longer be placed as transitions from the  $2^+$  (1517 keV) level to the  $2^+$  and  $3^+$  levels. The  $2^+_{K=0_3} \rightarrow 4^+$  transition still fits marginally in energy [energy discrepancy of 25(20) eV] but it is very unlikely that the  $2^+_{K=0_3} \rightarrow 4^+$   $E2$  transition would be 36(10) W.u. while the  $2^+_{K=0_3} \rightarrow 2^+$  transition would be  $\ll 1$  W.u. (most of the previous transition strength is now placed elsewhere). The Alaga rules would give, based on the  $2^+_{K=0_3} \rightarrow 4^+$  transition, a  $2^+_{K=0} \rightarrow 2^+$  transition of  $\sim 50$  W.u. or at least two orders of magnitude larger than the new upper limit of 1 W.u.

The 1517 keV level is therefore another case study in interpreting interband transitions. As with the  $K=0^+$  band, the apparent matrix elements of the 1517 keV level  $2^+_{K=0_3}$  to the  $\gamma$  band would seem very (in fact, too) collective. In the present case the explanation is not band mixing (as it is with the  $K=0^+$  band) but misplaced transitions in the existing level scheme.

It is remarkable that the authors of Ref. [17] correctly suspected, on the basis of their four-band mixing calculations, that their own  $\gamma$  placements for the 1517 keV level might be incorrect. The present data empirically confirms this and leads to the conclusion above that there is no positive evidence for multi-phonon character in the 1453 keV  $0^+$  excitation.

The third key result concerns the structure of negative parity excitations. Calculations in Ref. [18] predict that  $B(E1; K=0^- \rightarrow K=0^+_1)$  values are relatively strong and rather constant across the deformed rare earth nuclei:  $B(E1; 1^-_{K=0} \rightarrow 0^+_1)$  is  $7 \times 10^{-3} e^2 \text{ fm}^2$  to within a factor of 2 or so. In contrast, ground state  $E1$  transitions from the lowest  $K=1^-$  bands are predicted to fall off sharply (by 2–3 orders of magnitude) in going from Sm-Gd to Dy-Er-Yb. These predictions are shown in Fig. 3. In  $^{154}\text{Sm}$  and  $^{156}\text{Gd}$  the  $1^-_{K=1} \rightarrow 0^+_1 B(E1)$  values are predicted to be nearly comparable to the calculated  $B(E1; 1^-_{K=0} \rightarrow 0^+_1)$  values while they are predicted to be two orders of magnitude less

in heavier rare earth nuclei. While the decay data for  $K=0^-$  modes in rare earth nuclei are rather abundant, a  $B(E1)$  value for the  $1^-_{K=1} \rightarrow 0^+_1$  transition is known only in  $^{156}\text{Gd}$ . From Fig. 3 it is clear that  $^{158}\text{Gd}$  is the key transitional nucleus where the falloff is predicted to begin, and thus a measurement of  $B(E1)$  rates from the  $K=1^-$  band in this nucleus is an excellent first test of these predictions.

Our lifetime measurement for the  $1^-$  level at 977 keV in  $^{158}\text{Gd}$  provides the desired value, namely,  $B(E1; 1^-_{K=1} \rightarrow 0^+_1) = 0.000172 e^2 \text{ fm}^2$ . This value, the  $^{156}\text{Gd}$  value, and the experimental  $\Delta K=0$  results are included in Fig. 3. In providing the  $B(E1; 1^-_{K=1} \rightarrow 0^+_1)$  value in this pivotal nucleus (and only the second measured value in this mass region), these results do confirm the beginning of the predicted falloff in  $B(E1)$  values from  $K=1^-$  bands with increasing  $N$  and  $Z$  in the rare earth nuclei. However, they also suggest that the falloff occurs sooner and faster than predicted since the predicted value [18] is  $\sim 0.002 e^2 \text{ fm}^2$ , an order of magnitude larger than observed. The predicted ratio

$$\frac{B(E1; 1^-_{K=1} \rightarrow 0^+_1)}{B(E1; 1^-_{K=0} \rightarrow 0^+_1)} \sim 0.33$$

is also large compared to the experimental value of 0.07.

It is interesting to try to understand the microscopic origin of the behavior of these  $\Delta K=0$  and  $1 B(E1)$  values. The relative position of the two octupole vibrational bands can be understood in terms of the fractional filling of the shell [19,20]. In the beginning of the deformed region (e.g.,  $^{154}\text{Sm}$ ) the band sequence is  $K=0^-, 1^-$ . As the Fermi level increases, the sequence changes to  $1^-, 0^-$  [20], as in  $^{168}\text{Er}$ ,  $^{172}\text{Yb}$ .

In the absence of a detailed microscopic calculation, it is possible to invoke a simple ‘‘counting’’ analysis to at least provide clues to the behavior of the  $E1$  transition rates. Allowed  $E1$  transitions in the Nilsson scheme satisfy one of the following asymptotic selection rules on the Nilsson quantum numbers [21]

$\Delta K$	$\Delta N$	$\Delta \Lambda$	$\Delta n_z$
0	1	1	1
1	1	1	0

If one counts (for both protons and neutrons) the numbers of allowed transitions for nuclei with  $Z=50-82$  and  $N=82-126$ , one finds that there are nearly 50% more  $\Delta K=0$  cases than  $\Delta K=1$  cases. Moreover, whenever the  $E1$  matrix elements for both  $\Delta K=0$  and  $\Delta K=1$  transitions have a given quasiparticle orbit in common, the  $\Delta K=0$  case always corresponds to a lower quasiparticle energy difference. If we assume phase coherence among contributing amplitudes in the  $E1$  matrix elements, these two effects could easily account for a  $\Delta K=0-B(E1)$  value several times larger than the  $\Delta K=1$  values.

We can also use this kind of qualitative argument to understand the difference in relative  $\Delta K=0$  and  $1 B(E1)$  values in  $^{156}\text{Gd}$  compared to the Dy-Er-Yb nuclei. In the region of the Fermi energy for  $^{156}\text{Gd}$  there are (counting both protons and neutrons) about 11  $\Delta K=0$  allowed  $E1$  matrix elements, and about 6  $\Delta K=1$  cases. In contrast, for  $^{166}\text{Er}$  there

are 7  $\Delta K=0$  amplitudes and only 1  $\Delta K=1$ . Therefore, naively, it is plausible that the ratio of  $\Delta K=0$  to  $\Delta K=1-B(E1)$  values from  $K=0^-$  and  $1^-$  bands to the ground state band, respectively, should increase sharply from Gd to Er: that is, the relative  $\Delta K=1$   $B(E1)$  values should decrease. This is consistent with interacting boson approximation (IBA) model calculations [18] although it is not clear in what sense the macroscopic IBA can be “aware” of the number of microscopically allowed  $E1$  matrix elements.

In any case, the present  $^{158}\text{Gd}$  result concerns a pivotal nucleus where both IBA and a (simplistic) microscopic view suggest the beginning of a falloff in  $\Delta K=1$   $B(E1)$  values. It could be interesting to measure lifetimes for  $K=1^-$  states in the Er-Yb region to test whether the  $B(E1)$  values do fall off sharply in magnitude as predicted.

#### IV. CONCLUSIONS

The deformed nucleus  $^{158}\text{Gd}$  was studied to search for multiphonon  $K=0^+$  vibrational states and to study collective octupole states. The extraordinarily high energy precision and resolution of the GAMS4 spectrometer at the ILL in Grenoble has led to precise  $\gamma$  ray transition energies and lifetimes (via Doppler broadening on an eV scale) for levels

in  $^{158}\text{Gd}$ . We confirm the strong  $B(E2)$  values from the  $0_2^+$  band to the nearby  $\gamma$  band but noted that these can be explained, without invoking collective multiphonon states, via an existing [17] band mixing calculation. The high precision of GAMS4 revealed that previously assigned  $\gamma$  ray lines from the  $2^+$  (1517 keV) level of the second excited  $0^+$  band (at 1453 keV) were incorrectly placed. Again, this removed the existing evidence for multiphonon character here as well. Finally, measurements of  $B(E1:1^-K=1_1^- \rightarrow 0_1^+)$  values provided a rare example of  $E1$  transition strengths from  $K=1_1^-$  bands (many are known from  $K=0_1^-$  bands). The relatively large value obtained supports existing IBA calculations. These same calculations also point to a falloff in these  $B(E1:K=1^- \rightarrow K=0^+)$  values in heavier rare earth nuclei and therefore focus attention on the need for measurements in such nuclei.

#### ACKNOWLEDGMENTS

Work supported under U.S. DOE Contract Nos. DE-FG02-91ER-40609 and DE-FG02-88ER-40417. W. A. thanks the Bulgarian NRF for financial support under Contract No. PH511.

- 
- [1] M. Baranger, Phys. Rev. **120**, 957 (1960).
  - [2] R. F. Casten, J. Jolie, H. G. Börner, D. S. Brenner, N. V. Zamfir, W. T. Chou, and A. Aprahamian, Phys. Lett. B **297**, 19 (1992).
  - [3] H. G. Börner, J. Jolie, S. J. Robinson, B. Krushe, R. Piepenbring, R. F. Casten, A. Aprahamian, and J. P. Draayer, Phys. Rev. Lett. **66**, 691 (1991).
  - [4] W. Korten, T. Härtlein, J. Gerl, D. Habs, and D. Schwalm, Phys. Lett. B **317**, 19 (1991).
  - [5] C. Fahlander, A. Axelsson, M. Heinebrodt, T. Härtlein, and D. Schwalm, Phys. Lett. B **388**, 475 (1996).
  - [6] F. Corminboeuf, J. Jolie, H. Lehmann, K. Föhl, F. Hoyler, H. G. Börner, C. Doll, and P. K. Garrett, Phys. Rev. C **56**, 1201 (1997).
  - [7] P. E. Garrett, M. Kadi, C. A. McGrath, V. Sarokin, Min Li, Minfang Yeh, and S. W. Yates, Phys. Rev. Lett. **78**, 4545 (1997).
  - [8] R. D. Herzberg *et al.*, Nucl. Phys. **A592**, 211 (1995).
  - [9] N. Pietralla *et al.*, Phys. Rev. C **58**, 796 (1998).
  - [10] C. M. Bertulani, J. Phys. G **24**, 1165 (1998).
  - [11] M. S. Dewey, E. G. Kessler, G. L. Greene, R. D. Deslattes, H. G. Börner, and J. Jolie, Nucl. Instrum. Methods Phys. Res. A **284**, 151 (1989).
  - [12] H.G. Börner and J. Jolie, J. Phys. G **19**, 217 (1993).
  - [13] F. Becvar, Nucl. Instrum. Methods Phys. Res. A **417**, 434 (1998).
  - [14] R. G. Helmer, Nucl. Data Sheets **77**, 471 (1996).
  - [15] F. K. McGowan and W. T. Milner, Phys. Rev. C **23**, 1926 (1981).
  - [16] H. H. Pitz, U. E. P. Berg, R. D. Heil, U. Kneissl, R. Stock, C. Wesselborg, and P. von Brentano, Nucl. Phys. **A492**, 411 (1989).
  - [17] R. C. Greenwood *et al.*, Nucl. Phys. **A304**, 327 (1978).
  - [18] P. D. Cottle and N. V. Zamfir, Phys. Rev. C **54**, 176 (1996).
  - [19] R. F. Casten, W. T. Chou, and N. V. Zamfir, Nucl. Phys. **A555**, 563 (1993).
  - [20] K. Neegaard and P. Vogel, Nucl. Phys. **A145**, 33 (1970).
  - [21] B. R. Mottelson and S. G. Nilsson, Mat. Fys. Skr. Dan. Vid. Selsk **1**, No. 8 (1959).